TAMPERE UNIVERSITY OF TECHNOLOGY

Look-Up Table Based Implementation of Ultra-Low Complexity Narrowband OFDM Transmitters

Citation
Loulou, A., Yli-Kaakinen, J., Levanen, T., Lehtinen, V., Schaich, F., Wild, T., ... Valkama, M. (2019). Look-Up Table Based Implementation of Ultra-Low Complexity Narrowband OFDM Transmitters. In *2019 16th International Symposium on Wireless Communication Systems (ISWCS)* (pp. 127-132). (International Symposium on Wireless Communication Systems (ISWCS)). IEEE. https://doi.org/10.1109/ISWCS.2019.8877309

Year
2019

Version
Peer reviewed version (post-print)

Link to publication
TUTCRIS Portal (http://www.tut.fi/tutcris)

Published in
2019 16th International Symposium on Wireless Communication Systems (ISWCS)

DOI
10.1109/ISWCS.2019.8877309

Copyright
This publication is copyrighted. You may download, display and print it for Your own personal use. Commercial use is prohibited.

Take down policy
If you believe that this document breaches copyright, please contact cris.tau@tuni.fi, and we will remove access to the work immediately and investigate your claim.

Download date:07.03.2021

Look-Up Table Based Implementation of Ultra-Low Complexity Narrowband OFDM Transmitters

AlaaEddin Loulou*, Juha Yli-Kaakinen*, Toni Levanen*, Vesa Lehtinen*,
Frank Schaich†, Thorsten Wild†, Markku Renfors*, and Mikko Valkama*
*Electrical Engineering, Faculty of Information Technology and Communication Sciences, Tampere University, Finland
{alaa.loulou, juha.yli-kaakinen, toni.levanen, vesa.lehtinen, markku.renfors, mikko.valkama}@tuni.fi
†Nokia Bell Labs, Germany, {frank.schaich, thorsten.wild}@nokia-bell-labs.com

***Abstract*—In cyclic-prefix orthogonal frequency-division multiplexing (CP-OFDM) based radio access, the coexistence of different systems without precise time-frequency synchronization is limited due to high out-of-band emissions. Therefore, filtered-OFDM (F-OFDM) type spectrum enhancement can play a key role to relax the synchronization requirements as it provides well-contained spectrum through subband based filtering. This allows higher degree of flexible and dynamic spectrum use with minimized interference. However, this approach increases computational complexity compared with CP-OFDM. This paper presents a low-complexity solution for narrow-band F-OFDM transmitters based on the use of a look-up table (LUT) to store the F-OFDM waveform. This approach can be applied equally well for filtered version of the discrete Fourier transform-spread-OFDM (DFT-s-OFDM) waveform with small number of subcarriers. DFT-s-OFDM is commonly used in the uplink of OFDM-based systems to mitigate high peak-to-average power ratio (PAPR) of OFDM. The scheme is particularly interesting for the transmitters of Internet-of-Things (IoT) or massive machine type communication (mMTC) devices operating at low data rate. The LUT approach requires only memory units and relatively low number of additions. Moreover, we propose a low-complexity solution to deal with the CP-length variations within the transmission frame. The required memory wordlengths are evaluated through simulations. Comparisons with time-domain filtering and fast-convolution-based filtering solutions are included as well.**

***Index Terms*—NB-IoT, DFT-s-OFDM, filtered OFDM, multi-carrier waveforms, OFDM, look-up table, 5G New Radio.**

I. Introduction

The continuous development in the communication systems foresees the connection of all devices, such as home and industrial appliances, as an essential part of the future generation networks. This idea is widely known as Internet-of-things (IoT) or massive machine-type communication (mMTC) [1], [2]. A massive amount of devices is to be connected to the wireless network, transmitting/receiving sporadically messages with small payloads. The 3rd generation partnership project (3GPP) has introduced a new radio interface called narrow-band IoT (NB-IoT) mainly for long term evolution (LTE) networks. While NB-IoT is based on the LTE functionalities, it targets at ultra-low complexity devices with wide coverage, supporting mMTC devices with improved power efficiency [3]–[5]. NB-IoT can be deployed within the active resource blocks of the LTE system or within the guard-bands between active LTE resource blocks and channel edge; these are called in-band and guard-band deployment options. In the stand-alone option, NB-IoT channels can be deployed outside the LTE spectrum, e.g., on the global system for mobile communications (GSM) frequency bands. In all these options, the interference with coexisting technologies, such as GSM and LTE, should be minimized.

This work was supported by Business Finland and Nokia Bell Labs under the Wireless for Verticals (WiVe) project.

Both LTE and NB-IoT apply cyclic-prefix orthogonal frequency-division multiplexing (CP-OFDM) in the downlink. On the other hand, the uplink uses discrete Fourier transform-spread-OFDM (DFT-s-OFDM), also known as single-carrier frequency-division-multiple-access (SC-FDMA), in order to mitigate the peak-to-average power ratio (PAPR) of the transmitted signal. Generally, CP-OFDM and DFT-s-OFDM exhibit high-power spectral sidelobes potentially leaking to the neighboring parts of the spectrum. This is critical especially in the 5G New Radio (5G-NR), which extends the LTE numerology by allowing different subcarrier spacings (SCSs) in adjacent subbands. Such mixed numerology operation causes loss of OFDM subcarrier orthogonality. In order to reduce the interference leakage between subbands with different numerologies, 3GPP allows subband-based spectral enhancement techniques to be used, but these should be transparent to the receiver [6].

In NB-IoT, spectrum confinement is required to suppress the OFDM sidelobes in order to satisfy the out-of-band emission requirements of the 3GPP specifications [7]. The related difficulties in gurd-band and in-band deployments are discussed in [5], [8] and according to [8], the channel filtering challenges limit the deployment of NB-IoT with LTE carrier bandwidths smaller than 5 MHz. Effective NB-IoT filtering techniques can be expected to relax these issues. NB-IoT with some enhancements is also considered as one of the mMTC solutions for 5G [9]. In this context, the demands for NB-IoT subband filtering become more critical. Regarding uplink transmission, improved spectrum localization makes the system more tolerant to synchronization and power control imperfections. In summary, effective spectrum confinement techniques are needed for NB-IoT, both for satisfying the current specifications, and for enhanced performance and coexistence in NB-IoT evolution in the 5G-NR and beyond.

In the literature, various schemes have been proposed for OFDM spectrum enhancement. In 5G-NR development, a time-domain windowing approach, referred to as windowed overlap and add (WOLA) [10], and subband-wise filtered OFDM (F-

OFDM) [11]–[13] have been mainly considered. Generally, F-OFDM has better performance and higher complexity. F-OFDM is able to provide good spectrum localization for CP-OFDM physical resource blocks (PRBs) or groups of PRBs. Recently, the high flexibility and efficiency of fast-convolution (FC) based F-OFDM has been demonstrated in 5G-NR scenarios [14].

mMTC devices target at extremely low implementation complexity, and both time and frequency-domain digital filters may be considered too complex, as indicated also by the results below in Section IV. The WOLA technique [10] is able to satisfy 3GPP emission requirements, but it will compromise the link performance due to reduced effective CP length, and it lacks the potential of enhancing the spectrum localization beyond the current NB-IoT specifications.

In this paper, we propose an advanced implementation variant for F-OFDM and filtered DFT-s-OFDM (DFT-s-OFDM-F) with ultra-low complexity. It is suitable for narrowband uplink transmission, e.g., for the transmitter of an ultra-low cost mMTC device, requiring no multiplications. This new scheme stores the complex time-domain samples of the modulated symbols for each transmitted subcarrier or group of subcarriers in a look-up table (LUT) [15], [16]. Then the sample vector for transmission is selected from the LUT depending on the data symbols. This scheme avoids also the computationally complicated DFT/IFFT processing of DFT-s-OFDM, making it possible to do the digital waveform generation without any multiplications.

This paper is organized as follows. Section II gives first a short overview of NB-IoT and then presents a model for a DFT-s-OFDM-F transmitter. Section III proposes the new implementation variant for filtered CP-OFDM and DFT-s-OFDM signal generation using LUT, referred to as LUT-OFDM. In Section IV we compare the memory requirements and computational complexity of the LUT-OFDM and conventional DFT-s-OFDM-F. Then the memory wordlengths required to reach the 3GPP specifications of NB-IoT for in-band distortion and out-of-band emissions [7] are evaluated by simulations. Finally, concluding remarks are presented in Section V. Some essential notations are shown in Table I.

TABLE I
SYMBOLS AND NOTATIONS

Notation	Meaning
$W_i = \exp(-2\pi j/i)$	DFT twiddle factor, ith complex root of unity
$\mathbf{I}_i$	$i \times i$ identity matrix
$\mathbf{0}_{i\times p}$	$i \times p$ zero matrix
$\langle\cdot\rangle_i$	Modulo i operation
$\circ\mathbf{A}$	Element-wise power of matrix $\mathbf{A}$
B-DFT	DFT of length B

II. System Model

A. NB-IoT overview

The LTE standard uses CP-OFDM and DFT-s-OFDM schemes for downlink and uplink, respectively [17]. The standard offers a variety of bandwidth configurations from 1.4 MHz up to 20 MHz with 15 kHz SCS and 12 subcarrier PRB size. Considering LTE with frequency-division duplexing (FDD), time resources are divided into radio frames of 10 ms. Each frame is divided into 10 subframes, each of which is further divided into two slots. In the normal CP configuration, each slot contains 7 OFDM symbols, and the first CP is slightly longer than the other ones to maintain exactly 0.5 ms duration per slot. NB-IoT uses the LTE parameters with normal CP [5]. A NB-IoT channel uses up to 180 kHz of the spectrum. This is equivalent to one LTE PRB. For uplink, 1, 3, 6 or 12 subcarriers can be assigned to a UE with 15 kHz SCS while 3.75 kHz SCS with up to 48 subcarriers is also supported in single-tone transmission. Each transmission event uses at least one subframe with varying number of slots depending on the number of assigned subcarriers. In case of single subcarrier allocation (single-tone uplink), phase-rotated constellations $\pi/2$-BPSK and $\pi/4$-QPSK are used. In multi-tone transmission, only QPSK modulation is supported by the NB-IoT specifications, but BPSK modulation is also considered here for generality. The focus in this document is on the uplink side with 15 kHz SCS.

The NB-IoT baseband system model assumes that the 12 subcarriers of the PRB are located symmetrically around the zero-frequency (DC), i.e., the carrier frequencies are $(k+0.5)\Delta f$, where the subcarrier indices are $k = -6, -5, \ldots, 5$ and $\Delta f = 15$ kHz is the subcarrier spacing.

B. Filtered DFT-s-OFDM Transmitter Model

DFT-s-OFDM is an OFDM-based single-carrier transmission scheme, where each data symbol block of length B is first frequency-spread by a DFT of length B. Then the spread data is allocated to B contiguous subcarriers of an OFDM modulator that is implemented by inverse fast Fourier transform (IFFT). The complexity reduction in the DFT-s-F-OFDM based NB-IoT UE exploits the fact that the input bins of the IFFT are mostly unused (i.e., zero-valued). A CP of length N_{cp} is added to the IFFT output in the usual way. This is followed by the subband filtering process used to suppress the out-of-band sidelobes. We follow the uplink OFDMA baseband model, and a fixed lowpass filter, independent of used allocation, is utilized. The output signal is generated with significant oversampling, and the filter bandwidth corresponds to the channel bandwidth (180 kHz in the NB-IoT case).

Considering the varying CP length, the values of the CP length and other related parameters are defined as functions of the DFT-s-F-OFDM symbol index n, i.e., $N_{\mathrm{cp}}(n), N_{\mathrm{s}}(n)$, etc. Here $n = [0, 1, \ldots, N_{\mathrm{f}} - 1]$, N_{f} is the total number of DFT-s-F-OFDM symbols within a subframe, and $N_{\mathrm{s}}(n)$ is the length of the DFT-s-F-OFDM symbol that includes the length of the IFFT output samples N and CP samples $N_{\mathrm{cp}}(n)$.

The DFT-s-F-OFDM transmitter structure for a single input symbol is shown in Fig. 1. The actual output is the sum of waveforms produced by the B input symbols. The output of the block-wise filtering stage for a single input symbol (before overlap-add of the consecutive DFT-s-F-OFDM symbols which are extended by filtering) is

$$\mathbf{x}^{(b,n)}_{N_{\mathrm{c}}(n)\times 1} = \mathbf{f}^{(b,n)}_{N_{\mathrm{c}}(n)\times 1} a_{b,n}, \tag{1}$$

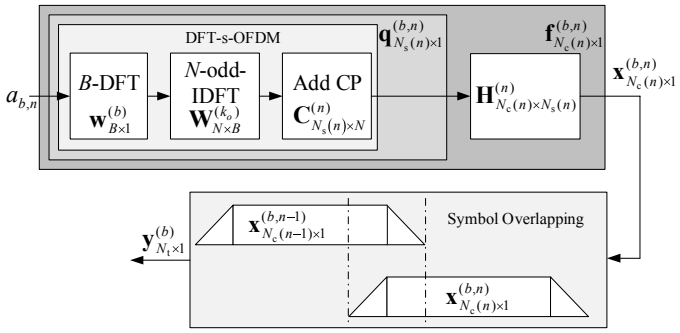

Fig. 1. The DFT-s-F-OFDM transmitter model for a single input symbol, used as a basis for developing the LUT scheme. The actual output is the sum of waveforms produced by the B input symbols.

where $a_{b,n}$ is the b^{th} input data symbol ($b = [0, 1, \ldots, B-1]$) of n^{th} DFT-s-F-OFDM symbol block. The length of the acyclic convolution of the DFT-s-F-OFDM symbol with the N_{h}-point impulse response is $N_{\text{c}}(n) = N_{\text{s}}(n) + N_{\text{h}} - 1$. In (1), $\mathbf{f}^{(b,n)}_{N_{\text{c}}(n)\times 1}$ is the DFT-s-F-OFDM processing vector expressed as:

$$\mathbf{f}^{(b,n)}_{N_{\text{c}}(n)\times 1} = \mathbf{H}^{(n)}_{N_{\text{c}}(n)\times N_{\text{s}}(n)} \mathbf{q}^{(b,n)}_{N_{\text{s}}(n)\times 1}. \tag{2}$$

Here, $\mathbf{H}^{(n)}_{N_{\text{c}}(n)\times N_{\text{s}}(n)}$ is the acyclic convolution matrix for low-pass filtering and $\mathbf{q}^{(b,n)}_{N_{\text{s}}(n)\times 1}$ is defined as

$$\mathbf{q}^{(b,n)}_{N_{\text{s}}(n)\times 1} = \mathbf{C}^{(n)}_{N_{\text{s}}(n)\times N} \mathbf{W}^{(k_o)}_{N\times B} \mathbf{w}^{(b)}_{B\times 1}, \tag{3}$$

where $\mathbf{w}^{(b)}_{B\times 1}$ is the spreading DFT vector of length B for the bth input expressed as

$$\mathbf{w}^{(b)}_{B\times 1} = \left[1, W_B^b, \ldots, W_B^{b(B-1)}\right]^T. \tag{4}$$

In (3), $\mathbf{W}^{(k_o)}_{N\times B}$ is a modified IDFT matrix with inputs of length B and k_o is the first (lowest) subcarrier of the allocation. It is convenient to assume the subcarrier index range of $[-N/2, N/2-1]$ while the IDFT length N takes a power-of-two value in practice. The matrix $\mathbf{W}^{(k_o)}_{N\times B}$ consists of the columns of the odd IDFT matrix corresponding to the used allocation,

$$\left(\mathbf{W}^{(k_{\text{o}})}_{N\times B}\right)_{(l+1)(b+1)} = W_N^{-l(k_{\text{o}}+b)} W_N^{-0.5l}, \tag{5}$$

where $l+1$ and $b+1$ are the matrix row and column indices and $l = 0, 1, \ldots, N-1$ is the output index of the N-odd-IDFT. Here the first term is the IDFT for the specific user allocation and the second term shifts the signal spectrum by half of the SCS. Depending on the system, the latter term may be absent, in which case (5) contains rows of the IDFT matrix.

In (3), $\mathbf{C}^{(n)}_{N_{\text{s}}(n)\times N}$ is the CP insertion matrix for the DFT-s-F-OFDM symbol that can be expressed as follows:

$$\mathbf{C}^{(n)}_{N_{\text{s}}(n)\times N} = \begin{bmatrix} \mathbf{0}_{N_{\text{cp}}(n)\times(N-N_{\text{cp}}(n))} & \mathbf{I}_{N_{\text{cp}}(n)} \\ & \mathbf{I}_N \end{bmatrix}. \tag{6}$$

The baseband signal for the whole subframe is created by using overlap and add for consecutive filtered symbols:

$$\mathbf{y}^{(b)}_{N_{\text{t}}\times 1} = \sum_{n=0}^{N_{\text{f}}-1} \mathbf{S}^{(n)}_{N_{\text{t}}\times N_{\text{c}}(n)} \mathbf{x}^{(b,n)}_{N_{\text{c}}(n)\times 1}. \tag{7}$$

Here $\mathbf{S}^{(n)}_{N_{\text{t}}\times N_{\text{c}}(n)}$ is a shift matrix that rearranges the DFT-s-F-OFDM symbols for overlap-and-add and it is expressed as

$$\mathbf{S}^{(n)}_{N_{\text{t}}\times N_{\text{c}}(n)} = [\,\mathbf{0}_{N_{\text{c}}(n)\times N_{\text{v}}(n)}\ \mathbf{I}_{N_{\text{c}}(n)}\ \mathbf{0}_{N_{\text{c}}(n)\times N_{\text{e}}(n)}\,]^T, \tag{8}$$

where $N_{\text{v}}(n)$ is the shift of the nth DFT-F-s-OFDM symbol,

$$N_{\text{v}}(n) = \sum_{r=0}^{n} N_{\text{s}}(r-1), \tag{9}$$

with $N_{\text{s}}(-1) = 0$ and $N_{\text{e}}(n)$ is the length of the remaining unused parts of the subframe that is defined as

$$N_{\text{e}}(n) = N_{\text{t}} - N_{\text{v}}(n) - N_{\text{c}}(n), \tag{10}$$

and N_{t} is the total number of the modulated samples in the subframe that is defined as follows:

$$N_{\text{t}} = \left(\sum_{n=0}^{N_{\text{f}}-1} N_{\text{s}}(n)\right) + N_{\text{h}} - 1. \tag{11}$$

In this section, a generic model for DFT-s-F-OFDM signal generation was formulated. For the NB-IoT case, we assume a symmetric transmission channel of 12 subcarriers around DC. Therefore, the half-subcarrier-shift was introduced in (5), following the 3GPP specifications [18]. This allows the use of a common real lowpass filter, with a bandwidth corresponding to the channel width, for all user allocations.

III. Look-up table based DFT-s-F-OFDM implementation

The structure of Fig. 1 includes all elements for baseband DFT-s-F-OFDM signal generation and it is used for generating table contents in LUT-based implementations. The following subsections first show the basic idea of LUT-OFDM, then the different variants of LUT-OFDM are introduced.

A. Basic input symbol based processing

Following the NB-IoT signal model, we consider basic and rotated binary and quaternary modulations. Let $d_{b,n}$ represent the data symbols, $d_{b,n} = [0, 1, \ldots, D-1]$, with $D = 2$ for binary and $D = 4$ for quaternary modulations. Then the complex input date symbols are of the form $a_{b,n} = (1+j)/\sqrt{2} \cdot (-1)^{d_{b,n}}$ for BPSK, $a_{b,n} = (1+j)/\sqrt{2} \cdot (-j)^{d_{b,n}}$ for QPSK, $a_{b,n} = j^{\langle n\rangle_2}(1+j)/\sqrt{2} \cdot (-1)^{d_{b,n}}$ for $\pi/2$-BPSK, and $a_{b,n} = \left((1+j)/\sqrt{2}\right)^{\langle n\rangle_2+1} \cdot (-j)^{d_{b,n}}$ for $\pi/4$-QPSK. The coefficients of these expressions, which are independent of the modulating symbol, can be combined with DFT-s-F-OFDM processing vector as follows:

$$\mathbf{m}^{(b,n)}_{N_{\text{c}}(n)\times 1} = \begin{cases} \left(\dfrac{1+j}{\sqrt{2}}\right) \mathbf{f}^{(b,n)}_{N_{\text{c}}(n)\times 1}, & \text{for BPSK \& QPSK} \\ \left(\dfrac{1+j}{\sqrt{2}}\right)^{\langle n\rangle_2+1} \mathbf{f}^{(b,n)}_{N_{\text{c}}(n)\times 1}, & \text{for } \pi/4\text{-QPSK} \\ j^{\langle n\rangle_2} \left(\dfrac{1+j}{\sqrt{2}}\right) \mathbf{f}^{(b,n)}_{N_{\text{c}}(n)\times 1}, & \text{for } \pi/2\text{-BPSK.} \end{cases} \tag{12}$$

As a result, it is possible to compute (12) and store the precomputed DFT-s-F-OFDM symbols in a look-up table. *In other words,* $\mathbf{m}^{(b,n)}_{N_{\text{c}}(n)\times 1}$ *contains all necessary processes for DFT-s-F-OFDM (i.e., DFT, IDFT, and filtering), which can be*

computed once and stored in the device memory. In the BPSK and QPSK cases, only a trivial phase rotation (corresponding to multiplication by $(-j)^{d_{b,n}}$) to be done in real-time. Eq. (12) contains an additional symbol index dependent phase rotation for both $\pi/2$-BPSK and $\pi/4$-QPSK. For $\pi/2$-BPSK, the phase rotation is a trivial multiplication that can be applied without the need to store different vectors for even and odd symbols, by slightly modifying the logic of the phase rotation. For $\pi/4$-QPSK, separate LUTs are needed for even and odd DFT-s-F-OFDM symbol indices in order to handle the needed $\pi/4$-rotations in a multiplier-free way. Consequently, the subcarrier overlap-and-add process in (7) is applied, resulting in DFT-s-F-OFDM structure without multiplications.

For the normal CP configuration, equal CP length is assigned for the symbols in a slot except for the first symbol, leading to two different lengths of the DFT-s-F-OFDM symbols. In precise implementation, different sample vectors should be stored for the two symbol lengths, approximately doubling the LUT size. However, it is possible to generate the filtered DFT-s-F-OFDM symbols approximately for symbols with longer CP from the stored sample vectors of the shorter symbol. With LTE numerology, the minimum IFFT length is $N = 128$, and this gives a natural choice for the sampling rate in NB-IoT signal generation. In this case, the CP length is 10 for the first symbol and 9 for the other ones. Our approach is just to shift the stored waveform by one sample when generating the first symbol of each slot. This corresponds to replacing the first sample of the longer CP by zero before filtering. In a way, the filtering extrapolates the missing sample from the CP, and we refer to this approach as *CP extrapolation*. It was verified by simulations that the effect of this approximation on the link performance is insignificant.

With the described approach, one sample vector needs to be stored for each input symbol index b in case of BPSK, QPSK, and $\pi/2$-BPSK and two sample vectors per symbol are needed for $\pi/4$-QPSK. Due to the DFT and IFFT processing, different sample vectors are usually needed for different symbol indexes within an input data block. Then $2B$ sample vectors need to be stored in the LUT for $\pi/4$-QPSK and B sample vectors are enough in the other cases. The length of the sample vectors comes from the (acyclic) convolution model as $N_{\mathrm{LUT}} = N + N_{\mathrm{CP}}(1) + N_{\mathrm{h}} - 1$, where N_{h} is the length of the filter impulse response. The generated partial waveforms need to be added together and then the overlapping parts of consecutive symbols need to be added up. The total number of complex additions per DFT-s-OFDM block is then approximately $(B-1)N_{\mathrm{LUT}} + N_{\mathrm{h}} - 1$ (assuming continuous transmission and ignoring the effect of CP extrapolation).

B. Input symbol grouping

The computational complexity (i.e, the number of additions) of LUT-OFDM can be reduced by processing the input symbols group-wise [15], [16]. Then the partial waveforms corresponding to all possible combinations of $d_{b,n}$ in the group are stored. The total number of alternative combinations is D^G where G is the number of input symbols in the group. If phase rotations are exploited, the number of alternatives can be reduced to $P = D^{G-1}$. Each possible combination is stored in the memory in such a way that it can be addressed using the symbol values $d_{b,n}$ with simple logic. Assuming that the input block size is divided into equal-sized groups, B/G sample matrices are needed, leading to the total number of sample vectors of $2B/G \cdot D^{G-1}$ for $\pi/4$-QPSK while $B/G \cdot D^{G-1}$ sample vectors are enough in the other cases.

TABLE II
PER ALLOCATION MEMORY REQUIREMENTS IN REAL SAMPLES FOR DIFFERENT LUT-OFDM VARIANTS IN NORMAL CP CONFIGURATION OF LTE WITH $N = 128$. THE MEMORY SIZES IN BOLD ARE CONSIDERED POTENTIALLY USEFUL IN PRACTICE.

Subband size	Group size	Short filter, $N_{\mathrm{h}} = 33$		Long filter, $N_{\mathrm{h}} = 120$	
		BPSK	QPSK	BPSK	QPSK
1	1	**338**	**676**	**512**	**1024**
3	1	**1014**	**1014**	**1536**	**1536**
	3	**1352**	**5408**	**2048**	**8192**
6	1	**2028**	**2028**	**3072**	**3072**
	3	**2704**	**10816**	**4096**	**16384**
	6	**10816**	346112	**16384**	524288
12	1	**4056**	**4056**	**6144**	**6144**
	3	**5408**	**21632**	**8192**	**32768**
	6	**21632**	692224	**32768**	1.0×10^6
	12	692224	1.4×10^9	1.0×10^6	2.1×10^9

IV. NUMERICAL RESULTS

A. Implementation complexity

Here we compare the memory requirements and computational complexity of different DFT-s-F-OFDM transmission schemes. The complexity of DFT-s-OFDM without filtering is used as a basic reference in all evaluated cases. The filtered DFT-s-OFDM schemes include the LUT-OFDM variants, as well as the and time-domain filtering scheme (DFT-s-OFDM-F) and fast-convolution filtering scheme (DFT-s-OFDM-FC). The schemes are tested using the transform size of $N = 128$ with the CP lengths of 10 and 9 samples for normal CP mode. Moreover, the $\pi/2$-BPSK and $\pi/4$-QPSK are used only for single-tone cases, while BPSK and QPSK are considered for multi-tone cases. Filter lengths of 33 and 120 are considered as extreme choices when searching for suitable performance vs. complexity trade-off. Regarding the non-LUT schemes, DFT-s-OFDM-F uses one transform of size 128 and time-domain filtering, while the DFT-s-OFDM-FC scheme contains three transforms of size 128, one IFFT for OFDM and the other two used for the FC filtering process [14].

Firstly, we focus on the coefficient memory requirements of different schemes. This is expressed in terms of memory words required for the real and imaginary parts of the coefficients of the non-LUT schemes and waveform samples in the LUT schemes. The bits per word requirements will be discussed below. The required memory for the coefficients of the non-LUT schemes are 61 memory units for DFT-s-OFDM, 63 memory units for DFT-s-OFDM-FC, and 160 or 421 memory units for DFT-s-OFDM-F with filter lengths of 33 or 120, respectively.

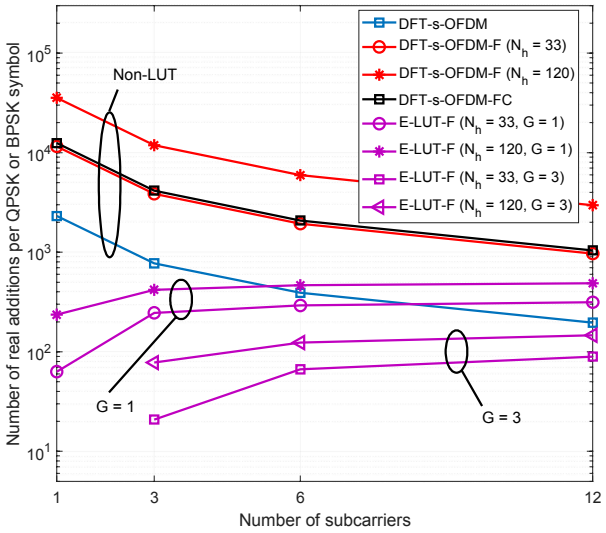

Fig. 2. Real addition rates per transmitted QPSK or BPSK symbol for the different DFT-s-OFDM schemes.

Table II shows the memory requirements for the different variants of LUT-OFDM with different allocation bandwidths and grouping arrangements using BPSK and QPSK. Here fixed allocations are assumed. The basic scheme, with different LUTs for different CP-lengths, is excluded from the table because the required memory is doubled with respect to the CP extrapolation case, while it was verified that the differences in link performance are marginal. The table shows significant differences in the memory usage between QPSK and BPSK. Moreover, the group size affects the memory requirements greatly. Groups of 12 subcarriers are completely unrealistic, while the group size of 6 might be considered feasible only with binary modulation.

Secondly, the normalized rates of real additions per QPSK or BPSK symbol with the filter lengths of 33 and 120 are shown in Fig. 2. The unrealistic group sizes of 6 and 12 are avoided. Apart from being multiplication free, LUT-OFDM variants reach lower addition rates than the filtered non-LUT schemes; in many cases even lower than basic DFT-s-OFDM.

B. LUT wordlength requirements

The LUT-OFDM schemes are implemented in fixed-point finite-wordlength arithmetic considering worst-case scaling, i.e., the signal is scaled in such way that overflows do not occur. We focus here on the NB-IoT case, for which the requirements for in-band and out-of-band (OOB) emissions and error-vector magnitude (EVM) are specified by 3GPP [7]. The baseband model is used in the simulations and the active subcarriers are allocated at the edge of the NB-IoT channel of 12 subcarriers, in which case the OOB emission requirements are the most challenging. The spectral simulations have been carried out using the signal length of 50 subframes. Besides, for LUT-OFDM and DFT-s-OFDM-F, a root raised cosine (RRC) filter with impulse response of length $N_\mathrm{h} = \{33, 120\}$, 180 kHz wide passband, and 30 kHz transition bands are used.

Fig. 3 shows the OOB emissions for basic and filtered DFT-s-F-OFDM and for LUT-OFDM with full-precision and quantized coefficients for single-tone and 12-tone cases, along with the 3GPP emission mask. The spectral characteristics are shown for QPSK modulation; with BPSK, the results are quite similar. Generally, the OOB emissions of the basic DFT-s-OFDM based NB-IoT are always higher than the OOB mask. Therefore, some additional signal processing is always required. Clearly, increasing the filter length increases the margin to the OOB emission mask. The non-quantized DFT-s-OFDM-F and 9 or 10 bit quantized LUT-OFDM satisfy the OOB emission requirements.

TABLE III
THE MINIMUM WORDLENGTHS REQUIRED TO REACH THE OOB AND IN-BAND EMISSIONS MASKS AND AT MOST 14 % EVM FOR DIFFERENT CP EXTRAPOLATION BASED LUT CONFIGURATIONS. THE RESULTS ARE FOR FILTER LENGTHS N_h = 33 (UPPER) AND N_h = 120 (LOWER NUMBERS).

Subband size	Group size	Wordlength limiting metric		
		OOB	In-band	EVM
1	1	10	4	5
		9	4	5
3	1	10	6	6
		10	5	6
	3	9	4	5
		9	4	5
6	1	10	7	6
		10	6	6
	3	9	5	6
		9	5	5
12	1	10	–	7
		10	–	7
	3	9	–	6
		10	–	6

The in-band emissions are measured from the unused subcarriers of the NB-IoT PRB, relative to the active subcarrier power, using an ideal DFT-s-OFDM receiver in noise-free case. For the EVM results, following the 3GPP specifications, the received symbols are equalized to reduce the distortion due to the non-ideal filter passband response. The major cause of in-band interference and increased EVM is the finite-wordlength implementation of the transmitter processing. 3GPP specifications allow 17.5 % (15.2 dB) EVM with BPSK and QPSK modulations. In order to leave room for other transmitter non-idealities, we target at 14 % (20 dB) maximum EVM due to quantization and filtering effects.

Table III shows the required LUT wordlengths to reach the 3GPP specifications for OOB and in-band emissions and EVM. It can be seen that the OOB emission mask is the most critical part of the specifications. The grouping of three subcarriers helps to reduce the minimum requirements by 1 bit in most of the cases. Generally, the resulting minimum wordlength is 9 or 10 bits.

It was also verified that CP extrapolation and LUT quantization to the OOB-based minimum wordlength have insignificant effects on the link performance in all tested configurations.

V. CONCLUSION

In this paper, efficient look-up-table (LUT) based schemes were developed for the digital baseband processing of the transmitters of narrowband IoT devices. The proposed scheme allows

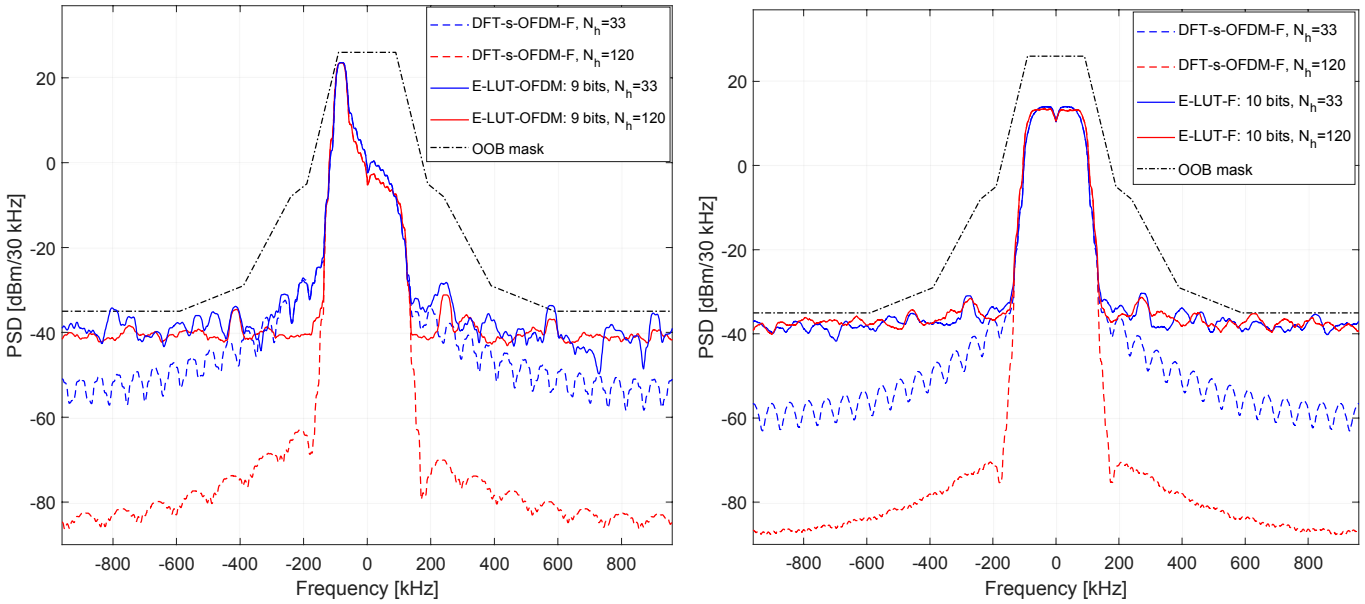

(a) (b)

Fig. 3. OOB emission for different DFT-s-OFDM transmitter schemes, including LUT schemes with 10 bit wordlength as well as non-quantized LUT and non-LUT cases, along with the 3GPP emission mask [7]. (a) Single-tone case with $\pi/2$-BPSK modulation. (b) 12-tone case with QPSK modulation.

ultra-low complexity on-line operation, after the complex evaluations of filtering and FFT/IFFT processes have been computed off-line and stored in the LUT. Based on matrix formalism for the filtered DFT-s-OFDM waveform, analytical expressions for the LUT computation were provided, along with expressions for the memory requirements and addition rates for different schemes. Multiplications can be completely avoided and addition rates are clearly reduced compared to the time-domain filtering and fast-convolution based schemes. By constructing the LUT for groups of subcarriers, the addition rate can be further reduced. A simple cyclic prefix (CP) extrapolation scheme was applied for reducing the memory requirements with variable CP lengths. Numerical comparisons were presented for different allocation bandwidths and group sizes, to identify configurations with reasonable memory requirements and addition rates.

While this work concentrated on NB-IoT framework, the proposed LUT-based schemes are applicable to any low-rate mMTC physical layer processing where additional filtering or windowing is required to improve the spectral containment of the transmitted signal.

An important topic for future work is to include a practical transmitter power amplifier model in the study.

REFERENCES

[1] D. Soldani and A. Manzalini, "Horizon 2020 and beyond: On the 5G operating system for a true digital society," *IEEE Vehicular Technology Magazine*, vol. 10, no. 1, pp. 32–42, Mar. 2015.

[2] J. Chen, K. Hu, Q. Wang, Y. Sun, Z. Shi, and S. He, "Narrowband internet of things: Implementations and applications," *IEEE Internet of Things Journal*, vol. 4, no. 6, pp. 2309–2314, Dec 2017.

[3] R. Ratasuk, N. Mangalvedhe, Y. Zhang, M. Robert, and J. P. Koskinen, "Overview of narrowband IoT in LTE Rel-13," in *Proc. 2016 IEEE Conf. on Standards for Communications and Networking (CSCN)*, Oct. 2016.

[4] Y. E. Wang, X. Lin, A. Adhikary, A. Grovlen, Y. Sui, Y. Blankenship, J. Bergman, and H. S. Razaghi, "A primer on 3GPP narrowband internet of things," *IEEE Com. Mag.*, vol. 55, no. 3, pp. 117–123, Mar. 2017.

[5] J. Xu, J. Yao, L. Wang, Z. Ming, K. Wu, and L. Chen, "Narrowband internet of things: Evolutions, technologies, and open issues," *IEEE Internet of Things Journal*, vol. 5, no. 3, pp. 1449–1462, Jun. 2018.

[6] T. Levanen, J. Pirskanen, K. Pajukoski, M. Renfors, and M. Valkama, "Transparent Tx and Rx waveform processing for 5G new radio mobile communications," *IEEE Wireless Communications*, vol. 26, no. 1, pp. 128–136, Feb. 2019.

[7] *User Equipment (UE) radio transmission and reception (Release 15)*, 3GPP TS 36.101, Mar. 2018, v15.2.0.

[8] R. Ratasuk, J. Tan, N. Mangalvedhe, M. H. Ng, and A. Ghosh, "Analysis of NB-IoT deployment in LTE guard-band," in *2017 IEEE 85th Vehicular Technology Conference (VTC Spring)*, June 2017.

[9] *Mobile IoT in the 5G future*, GSMA, Apr. 2018.

[10] R. Zayani, Y. Medjahdi, H. Shaiek, and D. Roviras, "WOLA-OFDM: A potential candidate for asynchronous 5G," in *Proc. 2016 IEEE Globecom Workshops (GC Wkshps)*, Dec. 2016, pp. 1–5.

[11] J. Abdoli, M. Jia, and J. Ma, "Filtered OFDM: A new waveform for future wireless systems," in *Proc. 2015 IEEE Workshop on Signal Proc. Advances in Wireless Comm. (SPAWC)*, Jun. 2015, pp. 66–70.

[12] V. Vakilian, T. Wild, F. Schaich, S. ten Brink, and J. F. Frigon, "Universal-filtered multi-carrier technique for wireless systems beyond LTE," in *Proc. IEEE Globecom Workshops (GC Wkshps)*, Dec. 2013, pp. 223–228.

[13] J. Li, E. Bala, and R. Yang, "Resource block filtered-OFDM for future spectrally agile and power efficient systems," *Physical Communication*, vol. 11, pp. 36 – 55, 2014.

[14] J. Yli-Kaakinen, T. Levanen, S. Valkonen, K. Pajukoski, J. Pirskanen, M. Renfors, and M. Valkama, "Efficient fast-convolution-based waveform processing for 5G physical layer," *IEEE Journal on Selected Areas in Communications*, vol. 35, no. 6, pp. 1309–1326, Jun. 2017.

[15] F. Schaich, T. Wild, R. Ahmed *et al.*, "Deliverable D3.1: Preliminary results for multi-service support in link solution adaptation," Project: Flexible Air iNTerfAce for Scalable service delivery wiThin wIreless Communication networks of the 5th Generation (FANTASTIC-5G), Tech. Rep., May 2016.

[16] F. Schaich and T. Wild, "Method of and apparatus for providing a sample vector representing at least a portion of a multi-carrier modulated signal," Patent application EP3 136 200A1, 2017.

[17] E. Dahlman, S. Parkvall, and J. Sköld, *4G: LTE/LTE-Advanced for Mobile Broadband (Second Edition)*. Oxford: Academic Press, 2014.

[18] *Technical Specification Group Radio Access Network (Release 15)*, 3GPP TS 36.211, Jun. 2018, v15.2.0.